

## THE IMPACT OF DIVALENT $\text{Co}^{2+}$ AND TETRAVALENT $\text{Zr}^{4+}$ TRANSITION METAL CATIONS ON STRUCTURAL, ELECTRICAL AND DIELECTRIC PARAMETERS OF $\text{MnFe}_2\text{O}_4$ NANOCRYSTALLINE SPINEL FERRITES FABRICATED VIA WET CHEMICAL ROUTE

A. FAISAL<sup>a</sup>, M. AKHTAR<sup>b,\*</sup>, M. A. KHAN<sup>c</sup>, A. WADOOD<sup>a</sup>

<sup>a</sup>Department of Chemistry, The Islamia University of Bahawalpur, Bahawalpur-63100, Pakistan

<sup>b</sup>Department of Chemistry, The Govt. Sadiq College Women University, Bahawalpur-63100, Pakistan

<sup>c</sup>Department of Physics, The Islamia University of Bahawalpur, Bahawalpur-63100, Pakistan

$\text{Mn}_{1-2x}\text{Zr}_x\text{Fe}_{2-y}\text{Co}_y\text{O}_4$  nano-ferrites were synthesized by micro-emulsion routine followed by structural elucidation by thermogravimetric analysis (TGA) and X-ray diffraction (XRD). TGA analysis revealed the phase formation temperature 950 °C and about 25 % weight loss was observed. This significant weight loss attributed to the use of surfactant molecules during synthesis. The synthesized nanoparticles of all compositions of  $\text{Mn}_{1-2x}\text{Zr}_x\text{Fe}_{2-y}\text{Co}_y\text{O}_4$  nano-ferrites were analysed by X-ray diffraction (XRD). The XRD confirmed the formation of face centered cubic spinel structure of doped and un-doped  $\text{MnFe}_2\text{O}_4$  nano-ferrites. The effect of dopants ( $\text{Co}^{2+}$  and  $\text{Zr}^{4+}$ ) on structural and dielectric parameters of manganese nano-ferrites has been investigated. The size of nano-ferrites, as determined by Scherrer formula was in the range of 30-75 nm. The nano-ferrites with crystallite size < 50 nm have significant signal to noise ratio and therefore they can be utilized in smart advanced technological electronic devices. The variation in the lattice parameters and crystallite size revealed an inhomogeneous change. This inhomogeneous behavior endorsed the replacement of higher ionic radii of  $\text{Zr}^{4+}$  on manganese site in the ferrite. The dielectric parameters were investigated up to 3GHz frequency range. A damping effect was observed in the dielectric constant, loss factor due to inclusion of Zr-Coin the Mn-ferrites.

(Received February 25, 2018; Accepted May 12, 2018)

*Keywords:* Spinel ferrite, Nanocrystallites, XRD, Dielectric, High frequency

### 1. Introduction

Nanoscience is relatively new branch of science. The researchers in the field of nanoscience belong to all disciplines and their main focus is to develop new smart but multifunctional materials. These multifunctional materials have applications in all areas of daily life i.e. ranging from energy related materials, catalysis, to the medical diagnosis and therapy. Among a variety of multifunctional nanomaterials, the ferrites are the iron oxide based materials which have magnetic properties. Ferrites are of several classes based on their structure. Spinel ferrites have the cubic structure with general formula  $\text{AB}_2\text{O}_4$  (A is divalent metal cation, B is trivalent  $\text{Fe}^{3+}$  ions).  $\text{MnFe}_2\text{O}_4$  is a spinel ferrite with several unique properties.  $\text{MnFe}_2\text{O}_4$  have been found in wide range of applications like in catalysis, biomedicine, absorbent, water treatment, magnetic fluid hyperthermia, cell separation and lithium ion batteries as well [1]. The judicious choice of particle size and size distributions and chemical composition can be used to tailor the electric, magnetic, catalytic and many other characteristics of  $\text{MnFe}_2\text{O}_4$  nano-ferrites [2]. Manganese ferrite nanoparticles are widely studied because of their particular properties of being moderate magneto-

\* Corresponding author: mehwish.akhtar@gscwu.edu.pk

crystalline and good dielectric behaviour[3]. Moreover Mn-ferrites have distinct properties like high resistivity and low losses as compare to other ferrites [4]. The structural and electrical properties of these nano-ferrites can be controlled to make them suitable for technological applications[5]. Ferrites can be synthesized by several techniques such as co-precipitation, hydrolysis, sol-gel method, hydro chemical etc. [6, 7]. The structure, surface properties and electric properties and magnetic properties depends on the composition of ferrites[8-10]. Metal ions having larger ionic radii change significantly structure, electric and magnetic properties [11-13]. Many investigations have been carried out so far to modify the properties of ferrites by doping in these ferrites [14].

In the present study, we have synthesized  $Mn_{1-2x}Zr_xFe_{2-y}Co_yO_4$  nano-ferrites by micro-emulsion method which are then characterized by various techniques. The main purpose of this study is to address the tailoring of structural and dielectric parameters of  $MnFe_2O_4$  nano-ferrites by simultaneous doping with two metal ions i.e.  $Zr^{4+}$  and  $Co^{2+}$ .

## 2. Experimental details

$Mn_{1-2x}Zr_xFe_{2-y}Co_yO_4$  ( $0.00 \leq x \leq 0.10$  and  $0.00 \leq y \leq 0.30$ ) nano-ferrites were prepared by micro-emulsion route [15, 16]. Following chemicals were used as received:  $Fe(NO_3)_2 \cdot 9H_2O$  (Merck-Germany, 99 %),  $MnCl_2 \cdot 4H_2O$  (98%, Beijing chemical works),  $Cl_2OZr \cdot 8H_2O$  (98%, Sigma-Aldrich),  $(CH_3COO)_2Co \cdot 4H_2O$  (98%, BDH), cetyltrimethylammoniumbromide (CTAB) (Bio Basic-Canada, 99%) and aqueous  $NH_3$  (BDH 35%). Briefly, required salt solution prepared in deionised water were mixed and stirred separately for each composition. CTAB was added as emulsifying agent, followed by increase in pH to 10-11 by freshly prepared 2 M aqueous ammonia. The precipitates were washed with deionised water and then dried. The grinded precipitates were annealed at  $950^\circ C$  using muffle furnace. The annealed  $Mn_{1-2x}Zr_xFe_{2-y}Co_yO_4$  nano-ferrites were then characterized by various experimental techniques.

## 3. Result and discussions

### 3.1 TGA analysis

TGA analysis of typical un-annealed sample was carried out using SDTQ600V8.2Build100 thermal analyzer. The heating rate was kept  $10^\circ C/min$ . The main purpose of the thermal analysis was to probe energy required for decomposition, oxidation dehydration or other chemical changes of materials. Further, the phase formation temperature of ferrite particles could also be estimated by this technique [17]. TGA/DTA curves are shown in Figure 1. This graph explained the weight loss in three steps. According to this graph the total weight loss is ~25%. At first step the observed weight loss is 4%, which is due to the removal of moisture contents. At second step the maximum weight loss is observed which is 11%. This is attributed to the decomposition of organic contents (CTAB) present in the samples. The weight loss is approximately 10% at third, which is due to the formation of oxides from hydroxides [18]. From TGA, the annealing temperature determined was  $950^\circ C$ , and at this temperature, all compositions of  $Mn_{1-2x}Zr_xFe_{2-y}Co_yO_4$  nano-ferrites were annealed.

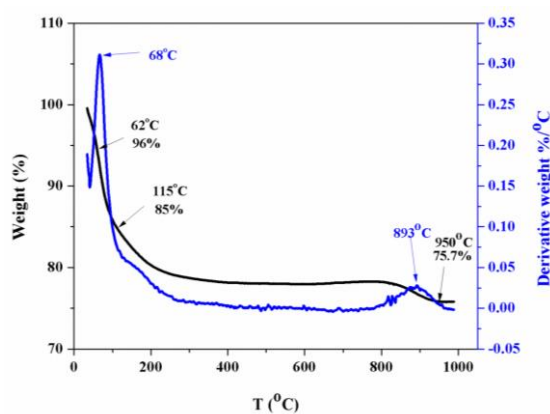


Fig. 1. Typical TGA / DTA curves of un-annealed- $Mn_{1-2x}Zr_xFe_{2-y}Co_yO_4$  nano-ferrites.

### 3.2 X-ray Diffraction (XRD)

All the annealed samples were characterized by XRD analysis in two theta range 10-80°. The XRD patterns of all compositions of  $Mn_{1-2x}Zr_xFe_{2-y}Co_yO_4$  nano-ferrites recorded at Philips X'Pert PRO 3040/60 diffractometer (with  $CuK\alpha$  as radiation source) are shown in Figure 2. The main reflections were compared with standard XRD patterns of  $MnFe_2O_4$  data card (01-074-2403) [19]. All the peaks in XRD patterns were matched with the standard XRD patterns of  $MnFe_2O_4$ . The phase centered cubic spinel structure of synthesized nano-ferrites was confirmed by XRD analysis.

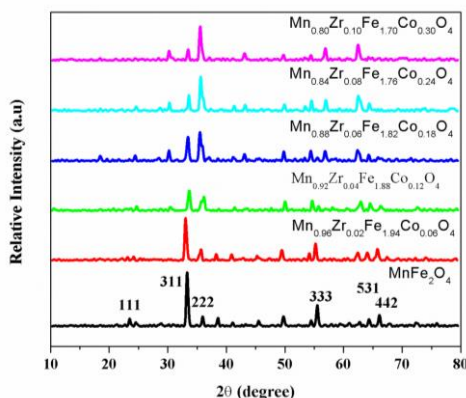


Fig. 2. XRD pattern of  $Mn_{1-2x}Zr_xFe_{2-y}Co_yO_4$  nano-ferrites.

The crystallite size of nano-ferrites was calculated by using Sherrer formula:

$$D = 0.9\lambda / \beta \cos\theta \quad (1)$$

In this equation, the “D” is the crystallite size,  $\beta$  is the full width at half maximum,  $\lambda$  is the value length of x-ray (1.5406 Å) and  $\theta$  is the angle of diffraction [20]. The crystallite size of nano-ferrites was found 30-75 nm (Table 1). The doping of Zr-Co produced small peaks near the main peak. The peak shifting was also observed due to the exchanged metal ionic radii. The value of lattice parameter (a) is calculated by using cell software. Cell volume is obtained by taking its cube. The results showed the increase in cell volume values with the increase in substitution. The decrease in the cell volume was also observed at  $x=0.04$  and  $x=0.10$ . The change in the lattice parameter (a) could be explained on the basis of difference in ionic radii of Co-Zr. The larger ionic radii of Co (0.72 Å) replaced the smaller ionic radii of  $Fe^{3+}$  (0.67 Å) [20]. On the other hand smaller ionic radii of  $Zr^{4+}$  (0.79 Å) [21] replaced the large ionic radii of  $Mn^{2+}$  (0.80 Å) [22]. The

increase in the values of lattice parameter (a) was due to the replacement of Fe<sup>3+</sup> by Co<sup>2+</sup> and decrease in the values was due to replacement of Mn<sup>2+</sup> by Zr<sup>4+</sup>. The lattice parameter (a) overall showed the increasing trend with the increase in dopant concentration which indicated the successful substitution.

Table 1. Cell parameters (a), cell volume and crystallite size for Mn<sub>1-2x</sub>Zr<sub>x</sub>Fe<sub>2-y</sub>Co<sub>y</sub>O<sub>4</sub> nanoparticles.

Parameters	x=0	x=0.02	x=0.04	x=0.06	x=0.08	x=0.10
	y=0.00	y=0.06	y=0.12	y=0.18	y=0.24	y=0.30
Lattice constant a/Å	8.5397	8.6248	8.6080	8.6694	8.6747	8.5740
Cell Volume/Å <sup>3</sup>	622.770	641.552	637.832	651.579	652.775	630.305
Crystallite Size/nm	62.82	54.99	73.35	44.25	31.60	73.74

### 3.3 Dielectric properties measurements

After structural elucidation, the Mn<sub>1-2x</sub>Zr<sub>x</sub>Fe<sub>2-y</sub>Co<sub>y</sub>O<sub>4</sub> nano-ferrites were subjected to dielectric parameters evaluation by impedance analyzer. The frequency of alternating current was kept 1 MHz to 3 GHz. From the obtained dielectric measurements, three main parameters (dielectric constant, dielectric loss and dielectrics loss tangent) were calculated and discussed. Dielectrics constant is used for the determinations of electrostatic energy stored per unit volume for unit potential gradient. In short dielectric constant is used to find out the charge storage ability of materials. It can be calculated by using this formula.

$$\varepsilon' = \frac{Ct}{\varepsilon_0 A} \quad (2)$$

In this equation  $\varepsilon'$  is the dielectric constant, C is the capacitance of the pellet, t is the thickness of the pellet, A represents the cross sectional area of the pellet and  $\varepsilon_0$  is the constant of permittivity for free space.

Dielectric loss factor is the imaginary part of relative dielectric permittivity. It is also called the measure of energy loss within the dielectric medium. The dielectric loss tangent can be calculated by using this equation.

$$\tan \delta = \frac{\varepsilon''}{\varepsilon'} \quad (3)$$

$\varepsilon''$  and  $\varepsilon'$  is the real and imaginary parts of dielectric constant[23].

Fig.3 shows the variation in dielectric constant with measuring frequency of applied ac field from 1 MHz to 3 GHz. It clearly shows the decrease in the value of dielectric constant with increasing frequency for all the samples. At initial stage the decrease in dielectric constant is much faster but became slower when reached in high frequency region and then it is not affected by the applied field. The observed behavior is due to space charge effect and can be explained on the basis of Maxwell-Wagner Model and Koops phenomenological theory.

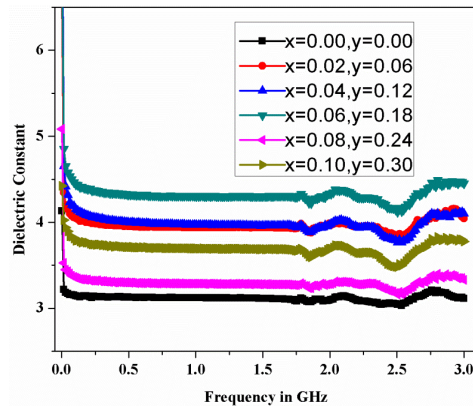


Fig. 3. Effect of frequency on the dielectric constant of  $Mn_{1-2x}Zr_xFe_{2-y}Co_yO_4$  nano-ferrites.

The grains present in dielectric medium are well conduction but the grain boundaries are poorly conducting therefore in low frequency region the effect of grain becomes dominant. In high frequency region the polarization becomes much slower than the applied ac field due to the charge carriers. At nearly 1.75 GHz the value of dielectric constant becomes minimum. However few peaks have been observed around 2 GHz to 2.5 GHz. These relaxations peaks are produced due to Debye- type relaxation, they also appeared when jumping frequency of  $Fe^{+2}$  and  $Fe^{+3}$  ions becomes exactly equal to the frequency of applied ac field [20]. Fig.3 shows that the value of dielectric constant increases as the Zr-Co concentration increased at high frequency. The dielectric constant value is minimum when Zr-Co contents were not substituted on the  $MnFe_2O_4$ . As the concentration of Zr-Co increases the value of dielectric also increased but at concentration  $x=0.08$  decreasing trend is observed which may be due to the inhomogeneity of sample. The values of dielectric constant with respects to frequencies and concentration at some selected frequencies are given in Table 2.

Table 2. Various dielectric parameters for " $Mn_{1-2x}Zr_xFe_{2-y}Co_yO_4$ " spinel ferrite.

Parameters	Frequency	x=0 y=0.00	x=0.02 y=0.06	x=0.04 y=0.12	x=0.06 y=0.18	x=0.08 y=0.24	x=0.10 y=0.30
Dielectric Constant	1.0 MHz	3.12	3.941	3.97	4.3	3.28	3.7
	1.5 GHz	3.11382	3.94004	3.95894	4.30243	3.28072	3.68829
	3.0 GHz	3.11241	4.04573	4.09848	4.45083	3.33022	3.77483
Dielectric Loss	1.0 MHz	1.324441	5.163743	7.647942	7.192322	3.852048	4.675263
	1.5 GHz	1.20727	4.69441	6.89651	7.0489	3.75507	4.59886
	3.0 GHz	8.3399	4.23498	3.5003	2.0846	4.03719	3.4785
tan $\delta$	1.0 MHz	4.245006	1.310421	1.927066	1.671598	1.172578	1.26525
	1.0 GHz	3.87713	1.19146	1.74201	1.63835	1.14459	1.24688
	3.0 GHz	2.6796	1.04678	8.5405	4.6836	1.21229	9.2148

The variations in dielectric loss with frequency for all compositions of  $Mn_{1-2x}Zr_xFe_{2-y}Co_yO_4$  nano-ferrite system at room temperature are shown in Figure 4. In low frequency region the decrease in dielectric loss is much faster but this reduction becomes slow with increase in frequency at last it becomes frequency independent in high frequency region. In low frequency region the grain boundaries produce high resistivity due to which energy is required for electron hopping and dielectric loss becomes very high. On the other hand in high frequency region less energy is required for electron hopping due to the high conductivity of grains. Dielectric loss depends on numbers of factors such as dopant contents, structural homogeneity, stoichiometry, which in turn depends on the composition and method of preparation. It is cleared from figure that by increasing the concentration of dopant the values of dielectric loss decrease but resistivity of samples increases [24].

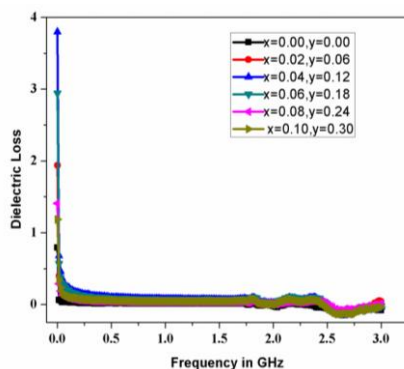


Fig. 4. Effect of frequency on the dielectric loss of  $Mn_{1-2x}Zr_xFe_{2-y}Co_yO_4$  nano-ferrites.

The relationship of dielectric loss tangent with the frequency for all compositions of  $Zr_xMn_{1-2x}Fe_{2-y}O_4Co_y$  nano-ferrites are presented in Figure 5. The dielectric loss tangent decreased with increasing frequency. The electrons follow the field when frequency of applied ac field becomes smaller as compared to hopping frequency of the electrons between  $Fe^{+2}$  and  $Fe^{+3}$  ions so the loss becomes maximum. On the other hand when the frequency of applied ac field becomes greater than hopping frequency, the electrons do not follow the field and loss becomes minimum. The Koops phenomenological theory proved that at low frequency of ac field the value of  $\tan \delta$  is higher and has a decreasing trend with increasing frequency. So the energy loss is greater at lower frequency region but it becomes smaller at high frequency region [25]. The  $\tan \delta$  produces when the polarization is much slower than the applied ac field. The inhomogeneity and impurities present in structures also cause the dielectric loss. If  $\tan \delta$  is less then it shows that samples are structurally homogeneous [26].

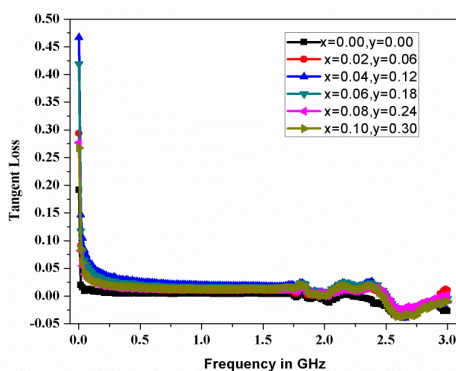


Fig. 5. Effect of frequency on the dielectric loss tangent of  $Mn_{1-2x}Zr_xFe_{2-y}Co_yO_4$  nano-ferrites.

#### 4. Conclusions

A series of  $Mn_{1-2x}Zr_xFe_{2-y}Co_yO_4$  ( $x=0.00, 0.02, 0.04, 0.06, 0.08, 0.10$  and  $y=0.00, 0.06, 0.12, 0.18, 0.24, 0.30$ ) were synthesized by micro-emulsion technique. X-ray diffraction (XRD) analysis confirmed the phase centered cubic spinel structure of prepared samples. TGA analysis showed about 25 % weight loss. By the substitution of Zr-Co, the lattice constant ( $a$ ) shows an increasing trend because, during this substitution the smaller ionic radii were replaced by large ionic radii. The dielectric constant and dielectric loss both showed a decreasing trend by the Zr-Co substitution. This happened because the effect of grain boundaries becomes dominant in low frequency region but in high frequency region the grain effect becomes dominant and polarization becomes much slower. So, all the samples show the normal dielectric behavior which suggests the utility of these nanomaterials in high frequency devices.

## Acknowledgements

Authors are thankful to The Islamia University of Bahawalpur, Bahawalpur-63100, Pakistan and The Govt. Sadiq College Women University, Bahawalpur-63100 Pakistan.

## References

- [1] G. Wang, Y. Ma, X. Dong, Y. Tong, L. Zhang, J. Mu, Y. Bai, J. Hou, H. Che, X. Zhang, *Applied Surface Science* **357**, 2131 (2015).
- [2] B. Antic, A. Kremenović, A.S. Nikolic, M. Stoiljkovic, *The Journal of Physical Chemistry B* **108**, 12646 (2004).
- [3] K. Vamvakidis, M. Katsikini, D. Sakellari, E. Paloura, O. Kalogirou, C. Dendrinou-Samara, *Dalton Transactions* **43**, 12754 (2014).
- [4] A. Jagminas, M. Kurtinaitienė, K. Mažeika **24**, 103 (2013).
- [5] N. Singh, A. Agarwal, S. Sanghi, P. Singh, *Journal of Magnetism and Magnetic Materials* **323**, 486 (2011).
- [6] T. Zare, M. Lotfi, H. Heli, N. Azarpira, A. Mehdizadeh, N. Sattarahmady, M. Abdollah-Dizavandi, M. Heidari, *Applied Physics A* **120**, 1189 (2015).
- [7] J. Jiang, Y.-M. Yang, L.-C. Li, *Physica B: Condensed Matter* **399**, 105 (2007).
- [8] M.F. Al-Hilli, S. Li, K.S. Kassim, *Journal of Magnetism and Magnetic Materials*, **324**, 873 (2012).
- [9] J. Jing, L. Liangchao, X. Feng, *Journal of Rare Earths* **25**, 79 (2007).
- [10] M. Shahid, M. Asghar, F. Malik, M. Warsi, *Journal of Ovonic Research* **13**, 143 (2017).
- [11] M.F. Al-Hilli, S. Li, K.S. Kassim, *Materials Chemistry and Physics* **128**, 127 (2011).
- [12] M. A. Iqbal, M. U. Islam, I. Ali, M.A. Khan, I. Sadiq, I. Ali, *Journal of Alloys and Compounds* **586**, 404 (2014).
- [13] M. Shahid, M. Rasheed, K. Fatima, A. Maryam, F. Malik, M. Asghar, M. Warsi, *Digest Journal of Nanomaterials & Biostructures (DJNB)* **12**, 1223 (2017).
- [14] C. Sun, K. Sun, *Solid State Communications* **141**, 258 (2007).
- [15] S. Kumar, V. Singh, S. Aggarwal, U.K. Mandal, R.K. Kotnala, *Materials Science and Engineering: B* **166**, 76 (2010).
- [16] R. Ali, M.A. Khan, A. Mahmood, A.H. Chughtai, A. Sultan, M. Shahid, M. Ishaq, M.F. Warsi, *Ceramics International* **40**, 3841 (2014).
- [17] W.J. Sichina, *Characterization of Polymers Using TGA*, Perkin Elmer instruments.
- [18] H. Sozeri, U. Kurtan, R. Topkaya, A. Baykal, M.S. Toprak, *Ceramics International* **39**, 5137 (2013).
- [19] M.A. Gabal, S.S. Ata-Allah, *Journal of Physics and Chemistry of Solids* **65**, 995 (2004).
- [20] R. Ali, A. Mahmood, M.A. Khan, A.H. Chughtai, M. Shahid, I. Shakir, M.F. Warsi, *Journal of Alloys and Compounds* **584**, 363 (2014).
- [21] Z. Wang, Z. Wang, W. Peng, H. Guo, X. Li, *Ceramics International* **40**, 10053 (2014).
- [22] M. Nirmala, A. Anukaliani, *Materials Letters* **65**, 2645 (2011).
- [23] M. Ajmal, PhD Thesis Pakistan, (2008).
- [24] B.P. Jacob, S. Thankachan, S. Xavier, E.M. Mohammed, *Journal of Alloys and Compounds* **578** 314 (2013).
- [25] M. Asif Iqbal, M.U. Islam, I. Ali, M.A. Khan, I. Sadiq, I. Ali, *Journal of Alloys and Compounds* **586**, 404 (2014).
- [26] R. Rani, G. Kumar, K.M. Batoo, M. Singh, *American Journal of Nanomaterials* **1**, 9 (2013).